Histological Study on the Possible Role of Platelet Rich Plasma in Repair of induced Acute Skeletal Muscle Injury in Adult Male Albino Rats

Original Article

Amy Mohamed Ahmed[1]; Sahar Gamal Abo Elfadl[1,2]; Dalia Ibrahim Ismail[1] and Soheir Assaad Filobbos[1]

[1]*Department of Histology, Faculty of Medicine, Cairo university, Cairo, Egypt*

[2]*Department of Medical Histology, College of Medicine, Misr University for Science & Technology (MUST)*

ABSTRACT

Introduction: Musculoskeletal injuries are widespread causes of sport injuries. Ordinary therapy is inadequate for rapid healing. So, in this study, the therapeutic effects of platelet rich plasma (PRP) were investigated as it is simple, efficient, and minimally invasive, and lessen recovery time.

Materials and Methods: Fifty-four adult male albino rats, were categorizes into four groups: Group I (control group). Group II had a crush injury to the right gastrocnemius muscle, then sacrificed after 2 hours. Group III received no treatment and were subdivided into subgroups III A and III B, each includes 6 rats sacrificed after 7 and 14 days, respectively. Group IV, were injected immediately after injury by 0.1 ml PRP in injury site, then were subdivided into subgroups IV A and IV B, each includes 6 rats sacrificed after 7 and 14 days, respectively. Blood samples were analyzed for serum creatine phosphokinase (CPK) level. Sections from the middle part of the right gastrocnemius muscle were processed for histological assessment using H. and E., Masson trichrome stain, immunohistochemical staining for myogenin immunoreactivity, in addition to semithin and ultra-thin sections for light and electron microscopic examination, followed by morphometric and statistical studies.

Results: Sections of group II showed disorganized, fragmented, discontinued, and tapering muscle fibers, disrupted Z discs at focal areas and giant disfigured mitochondria. The CPK level and mean number of myogenin immunoreactive nuclei and mean area percent of fibrous tissue were elevated, while the mean diameter of muscle fibers was decreased versus the control. Group III showed partial improvement, significant decrease in CPK level and increase in mean area percent of fibrous tissue, mean number of myogenin immunoreactive nuclei and in fiber diameter. Group IV showed prominent improvement.

Conclusion: Platelet rich plasma could enhance repair of acutely crushed skeletal muscle and accelerate the healing process with minimal fibrosis.

Received: 09 March 2023, **Accepted:** 19 April 2023

Key Words: Masson trichrome, muscle injury, myogenin, platelet rich plasma, satellite cells.

Corresponding Author: Amy Mohamed Ahmed, PhD, Department of Histology, Faculty of Medicine, Cairo university, Cairo, Egypt , **Tel.**: +20 10 9750 1202, **E-mail:** amy.ahmed@kasralainy.edu.eg

ISSN: 1110-0559, Vol. 47, No. 2

INTRODUCTION AND AIM OF THE WORK

Skeletal muscle injuries are the commonest cause of a significant pain as well as disability, making them a difficult issue for traumatology. These injuries are responsible for sports-related injuries. Recovery with traditional therapy, is usually insufficient. This has sparked a lot of interest in the possibility of new technologies like PRP, to speed up the healing process and reduce recovery time[1,2].

Therapies using PRP has gained increasing scientific interest for their ability in enhancing the healing of these injuries. They offer the ability to manipulate tissue healing[3]. PRP is used for the treatment of tendon lesions[4], skin rejuvenation[5] and treatment of cartilage lesions[6].

Platelet rich plasma is plasma volume with higher concentration of platelets than normal blood levels, delivering autologous blood product that can be injected into any injured part of the body to aid healing[7]. In addition, it is a technique that is low-cost, safe, and simple to use with a high capacity for regeneration, making PRP promise for cure of muscle injuries[8].

A transcription factor is encoded by the particular skeletal muscle gene known as myogenin. It controls the fusing of myoblasts throughout development. In rapidly diffusing satellite cells during myogenic differentiation during muscle regeneration, myogenin expression is increased[9,10].

That is why the present work aimed at studying the possible role of PRP in repairing induced acute skeletal muscle crush injury in rats.

Personal non-commercial use only. EJH copyright © 2024. All rights served *DOI: 10.21608/ejh.2023.199071.1870*

MATERIALS AND METHODS

MATERIALS

A. Drugs

For anesthesia a cocktail of ketamine chlorhydrate 60 mg/kg (Pfizer pharmaceuticals, Egypt) and xylazine 15 mg/kg (Adwia pharmaceuticals, Egypt) was administered intra-peritoneally (i.p.)[11] just before trauma induction.

B. Platelet-rich Plasma preparation

This research was conducted at Cairo University's Biochemistry Department of the Faculty of Medicine. Five milliliters of blood were taken from each rat's tail vein and placed in vacuum tubes with 10% sodium citrate as an anticoagulant. PRP was then made using the double centrifugation method outlined by Sonnleitner *et al* (2000)[12]. According to experimental procedure, each rat was injected by 0.1 ml of PRP at injury site[11].

C. Animals

Fifty four adult male albino rats, on average weighing 200 grams and roughly three months old, participated in the current investigation. They were kept in the Kasr El-Aini Faculty of Medicine's animal house, where they were given care according to standards endorsed by the Institutional Animal usage Care and Use Committee (CU-IACUC), approval number CU III F 49 19. Throughout the acclimatization week and the experimental period, animals were kept in stainless steel cages with standard diets and free access to standard water and air.

EXPERIMENTAL PRCEDURE

Trauma Model

A single impact blunt trauma caused by a metal mass (0.5 kg) descending through a guide from a height of 18 cm on the middle third of the right gastrocnemius muscle belly was performed under anesthesia[13].

Group I (Control group): Subgroup IA: included 18 rats, they were neither exposed to trauma nor to PRP injection, equally subdivided into 3 subgroups. Six rats were sacrificed on 0^{th} day, 7^{th} day and 14^{th} day, respectively.

Subgroup IB: included 6 rats injected with 0.1 ml PRP in right gastrocnemius without induction of trauma.

Group II (Trauma group): Group II: included 6 rats that had a crush injury to the right gastrocnemius muscle under anesthesia. Two hours later, they were sacrificed.

Group III (Spontaneous recovery group): included 12 rats that were subjected to crush injury under anesthesia to the right gastrocnemius. Then, they were divided equally and randomly to:

Subgroup IIIA: they were sacrificed after 7 days.

Subgroup IIIB: they were sacrificed after 14 days.

Group IV (Treated group): included 12 rats that were subjected to crush injury under anesthesia to the right gastrocnemius. Then, they were injected by 0.1 ml PRP in the right gastrocnemius injury site immediately after injury. Later, they were divided equally and randomly to:

Subgroup IVA: they were sacrificed after 7 days[11].

Subgroup IVB: they were sacrificed after 14 days[14].

METHODS

Creatine phosphokinase (CPK) levels

After each trial, blood samples were taken from the tail vein right before the animal was sacrificed. At Cairo University's Biochemistry Department in the Faculty of Medicine, samples were examined for CPK.

Histological study

Rats were sacrificed under anesthesia by Intra-peritoneal injection of phenobarbital (80mg/kg)[15]. The specimens from the middle part of the right gastrocnemius muscle were dissected and excised. It was divided into two specimens:

A. The first specimen: Specimen was fixed in 10% buffered formalin saline for 24 hours, dehydrated in ascending grades of ethanol and embedded in paraffin. Serial longitudinal sections of 5 µm were cut and subjected to the following:

1. Hematoxylin & eosin (H. and E.) stain[16].
2. Masson’s trichrome to detect fibrous tissue[17].
3. Immunohistochemical study[17].

Anti-Myogenin antibody (#YPA2269A): Rabbit polyclonal antibody (Chongqing Biospes Co., Ltd, china). The bound primary antibody was immunodetected using the labeled avidin-biotin- peroxidase complex (Histostain SP kit, Zymed Laboratories Inc, San Francisco, USA). Diaminobenzidine (DAB) was used as a chromogen and Meyer's haematoxylin as a counterstain. To establish immunohistochemical staining specificity, negative control serial sections were processed by replacing the primary antibody by phosphate buffer saline with all other steps performed in the same manner. Positive tissue control for myogenin immunostaining was human rhabdomyosarcoma with a brownish nuclear reaction.

B. The second specimen: Right gastrocnemius specimens were preserved in glutaraldehyde and embedded in resin. Toluidine blue was used to stain semithin sections[17], which were subsequently viewed under a light microscope with a 100X oil immersion lens. Using an ultramicrotome and diamond knife, extremely thin sections (60–80 nm) were cut, and then they were put on copper grids. After 30 minutes of saturation uranyl acetate staining in 50% ethanol and repeated washes with distilled water, the sample was stained for 5 minutes with lead citrate. At the Cairo University Research Park's electron microscope unit, analysis was completed using a transmission electron microscope (T.E.M.) JEOL (JEM-1400 Electron Microscope) (CURP). In each section, ten fields were examined.

Morphometric Study

Using Leica Qwin 500 LTD (Cambridge UK) computer assisted image analyzer, the following parameters were measured at the Histology Department, Faculty of Medicine, Cairo University.

1. Area percent of fibrous connective tissue stained with Masson trichrome.
2. Number of cells stained with myogenin antibody: Interactive counting of the immunopositive cells was performed for each section at x400 magnification.
3. Diameter of skeletal muscle fibers was measured in all H. and E.-stained sections at x200 magnification.

Statistical Analysis

The SPSS program version 21 was used for the CPK enzyme and morphometry. One-way analysis of variance (ANOVA)is used to compare and summarize quantitative data in the form of means and standard deviations. A post hoc Tukey test is conducted after any significant ANOVA to determine which pairings of groups contributed to the significant difference. Statistical significance is defined as a *P-value* of 0.05 or lower[18].

RESULTS

Laboratory Results

Creatine Phosphokinase (CPK) Results (Histogram 1)

The mean value of CPK level in group I (123.9±0.99) was the lowest among all other groups. Mean value of CPK of group II (330±9.6) was the highest among all other groups. After 7 days, the mean value of CPK in subgroup IIIA (302.3±3.77) was significantly higher than subgroup IVA (255±7.68). While, after 14 days, subgroup IIIB (204±4.1) was significantly higher than subgroup IVB (154.7±3.65). And was significantly lower than subgroup IIIA after 7 days. On the other hand, subgroup IVB was significantly lower than subgroup IVA after 7 days.

Histological Results

Hematoxylin and Eosin Results

Subgroup IA and subgroup IB showed similar histological features. Therefore, results of subgroup IA are demonstrated. In longitudinal section (LS), the muscle fibers appeared cylindrical, parallel, and of uniform thickness. Also, they revealed peripheral multiple oval nuclei. Fibers were separated by connective tissue (CT) endomysium (Figure 1A). Histological examination of LS of gastrocnemius muscle sections of group II (Trauma group) revealed disorganized, fragmented, discontinued, and tapering muscle fibers. The connective tissue endomysium appeared widened and contained apparently numerous CT fibers and cells (Figure 1B).

Subgroup IIIA (Spontaneous recovery group) after 7 days, revealed irregularly arranged fibers with frequent splitting, CT showed excessive fibrous tissue with mononuclear cellular infiltration (Figure 1C). After 14 days, subgroup IIIB showed muscle fibers with relatively apparent small diameter. Connective tissues between muscle fibers showed extensive regular fibrosis (Figure 1D).

While Subgroup IVA (Treated Group) after 7 days showed regularly arranged muscle fibers. Connective Tissue showed inflammatory cellular infiltrate and dilated congested blood vessels (Figure 1E). Histological examination of LS of gastrocnemius muscle sections of subgroup IVA showed parallel regularly arranged muscle fibers with peripherally arranged flat nuclei and occasional row of central nuclei (Figure 1F).

Masson's Trichrome Results

Longitudinal sections of subgroup IA showed cylindrical parallel muscle fibers of uniform thickness separated by minimal amount of CT endomysium (Figure 2A). While group II showed disorganized fragmented and discontinued muscle fibers. The Connective tissue endomysium appeared increased and contains extravasated red blood cells and collagen fibers (Figure 2B).

Subgroup IIIA after 7 days showed increased areas of fibrous tissue endomysium between muscle fibers (Figure 2C). After 14 days subgroup IIIB showed large amount of fibrous tissue between disorganized muscle fibers (Figure 2D).

While subgroup IVA after 7 days showed minimal fibrous connective tissue between muscle fibers (Figure 2E). Meanwhile subgroup IVB after 14 days showed minimal fibrous tissue between well-organized muscle fibers in most of the examined fields (Figure 2F).

Immunohistochemical Results for Myogenin

Examination of sections obtained from subgroup IA showed negative nuclear immunostaining of myogenin in the vicinity of muscle fibers (Figure 3A). Group II showed occasional brown immuno-stained reaction in the nuclei around the muscle fibers (Figure 3B).

Subgroup IIIA after 7 days showed some immuno-stained reaction in the nuclei around the muscle fibers (Figure 3C). After 14 days subgroup IIIB showed many immuno-stained reaction in the nuclei around the muscle fibers (Figure 3D).

Subgroup IVA after 7days showed many immuno-stained nuclei around the muscle fibers (Figure 3E). While subgroup IVB after 14 days showed large number of immuno-stained nuclei around the muscle fibers (Figure 3F).

Semithin Sections Results

Longitudinal sections, from subgroup IA showed parallel muscle fibers with regular transverse striations as well as peripheral flat vesicular nuclei having prominent

nucleoli (Figure 4A). Group II showed fragmented and discontinued muscle fibers. Blood capillaries with leucocytes in their lumen mainly basophils and macrophages appeared in increased CT (Figure 4B).

Subgroup IIIA after 7 days revealed discontinued tapering muscle fiber with loss of transverse striations in some areas. Connective tissues endomysium showed excessive wavy collagen bundles and flattened oval cells nuclei of fibroblasts (Figure 4C). After 14 days, subgroup IIIB showed muscle fibers with loss of striations in some areas, together with nuclei with irregular outline and paler compared to control. Extensive fibrosis was seen in CT between muscle fibers with appearance of inflammatory cells as mast cells (Figure 4D).

While subgroup IVA after 7 days revealed some muscle fibers with narrower diameter, central nuclei, and transverse striations (Figure 4E). Meanwhile subgroup IVB revealed regularly arranged muscle fibers with transverse striations, festooned sarcolemma, and peripheral flat vesicular nuclei with prominent nucleoli (Figure 4F).

Ultra-thin sections results

Longitudinal sections of group IA showed myofibrils with alternating and light bands. Each A band has a central H zone bisected by M line. Each I band was bisected by a Z disc. Sarcoplasm contained numerous intermyofibrillar mitochondria (Figure 5A). Group II showed discontinued muscle fibrils with disorganized myofibrils. Occasional disrupted or completely lost Z discs appeared at focal areas. Giant disfigured mitochondria appeared among the myofibrils (Figure 5B).

Subgroup IIIA After 7 days showed occasional discontinued muscle fibrils, lost Z line and distorted mitochondria. Some other fibers appeared with intact Z line (Figure 5C). After 14 days subgroup IIIB showed regular arrangement of muscle fibrils with intact Z lines in some areas, while other areas show disorganized myofibril arrangement with disrupted Z line. Mitochondria appeared disfigured and giant (Figure 5D).

While subgroup IVA after 7 days showed intact Z lines in fibrils. Discontinued muscle fibrils were still recognized with many mitochondria between fibrils. Some areas were still showing complete dissolution (Figure 5E). While subgroup IVB after 14 days showed regular arrangement of muscle fibrils with intact Z line in some areas, while other areas still show disorganized myofibril arrangement with disrupted Z line. Mitochondria appeared disfigured and giant (Figure 5F).

Quantitative Morphometric Results

Masson's Trichrome Area Percent Results (Histogram 2)

The mean value of Masson's trichrome area percent in group I (2.5±0) were the lowest among all other Groups. Group II (3.8±0.51) was higher than Group I.

After 7 days, the mean value of Masson's trichrome area percent in subgroup IIIA (6.5±0.52) was significantly higher than subgroup IVA (3.5±0.52). While, after 14 days, subgroup IIIB (10.5±0.52) was higher than subgroup IVB (4.5±0.52) and significantly higher than subgroup IIIA after 7 days. On the other hand, after 14 days, the mean value of Masson's Trichrome area percent in subgroup IVB was of higher significance than subgroup IVA after 7 days.

Mean Number of Positive Myogenin Immunoreactive Nuclei (Histogram 3)

Group I (0.1±0.316) was the lowest among all other Groups. While group II (1.5±0.52) was higher than group I

After 7 days, subgroup IIIA (2±0.81) was significantly lower than subgroup IVA (4±0.81). While, after 14 days, subgroup IIIB (4.5±0.52) was significantly lower than subgroup IVB (5.7±0.82)

After 14 days, subgroup IIIB was significantly higher than subgroup IIIA after 7 days while subgroup IVB was significantly higher than group IVA after 7 days.

Mean Diameter of Muscle Fibers in LS

Group I (37.8) was the significantly higher than group II (21.1±5.54). After 7 days, subgroup IIIA (28.6±4.5) was significantly lower than subgroup IVA (35.8±1.61). While, after 14 days, subgroup IIIB (31.2±1.34) was significantly lower than subgroup IVB (35.6±6.05) and higher than subgroup IIIA after 7 days.

After 14 days, subgroup IVB was significantly higher than subgroup IVA after 7 days (Histogram 4).

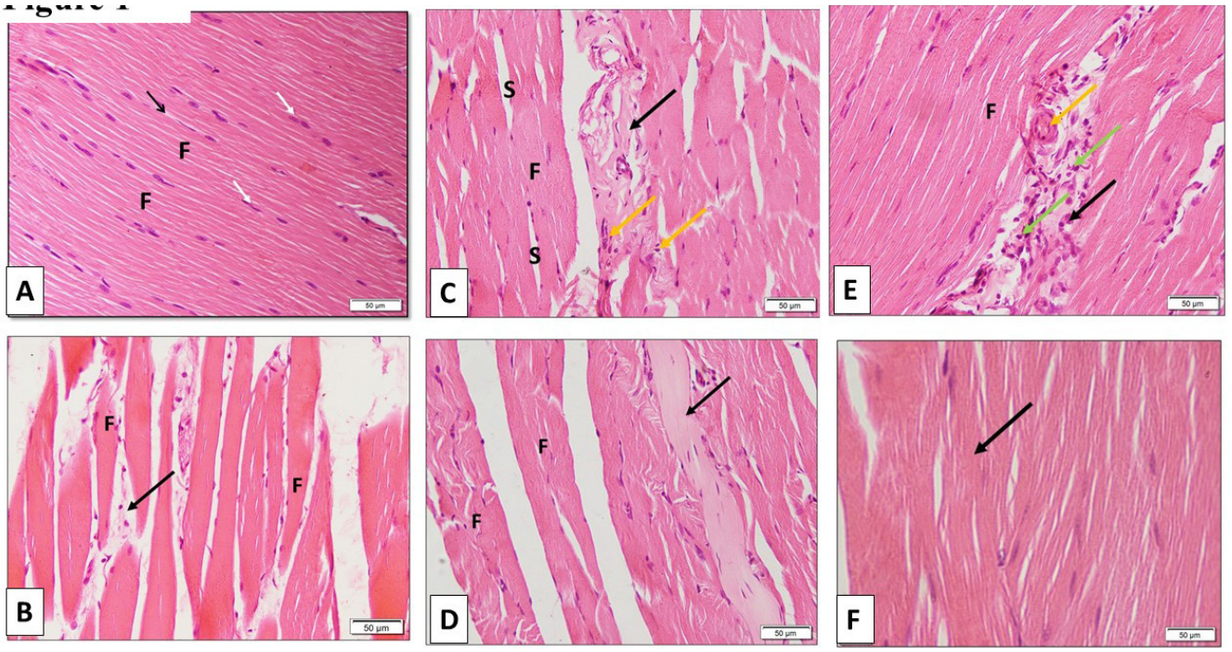

Fig. 1: Photomicrographs of a longitudinal section of an albino rat gastrocnemius muscle stained with H. and E. (x200). (1A) group I (Control group) showing cylindrical parallel muscle fibers (F) of uniform thickness separated by connective tissue endomysium (black arrow). Peripheral flat nuclei are noted (white arrows). (1B): Group II (Trauma group) showing disorganized, fragmented, discontinued, and tapering muscle fibers (F). The connective tissue endomysium (black arrow) appears widened and contains numerous CT fibers and cells. (1C): Subgroup IIIA (Spontaneous recovery group after 7 days) showing irregularly arranged muscle fibers (F) with frequent splitting (S). Connective tissue (black arrow) shows excessive fibrous tissue with mononuclear cellular infiltration (yellow arrows). (1D): Subgroup IIIB (Spontaneous recovery group after 14 days) showing some muscle fibers with relatively small diameter (F). Connective tissue between muscle fibers shows extensive regular fibrosis (black arrow). (1E): Subgroup IVA (Treated group after 7 days) showing regularly arranged muscle fibers (F). Connective tissue (black arrow) shows inflammatory cellular infiltrate (green arrows) and a thickened blood vessel (yellow arrow). (1F): Subgroup IVB (Treated group after 14 days) Longitudinal section shows parallel regularly arranged muscle fibers (black arrow).

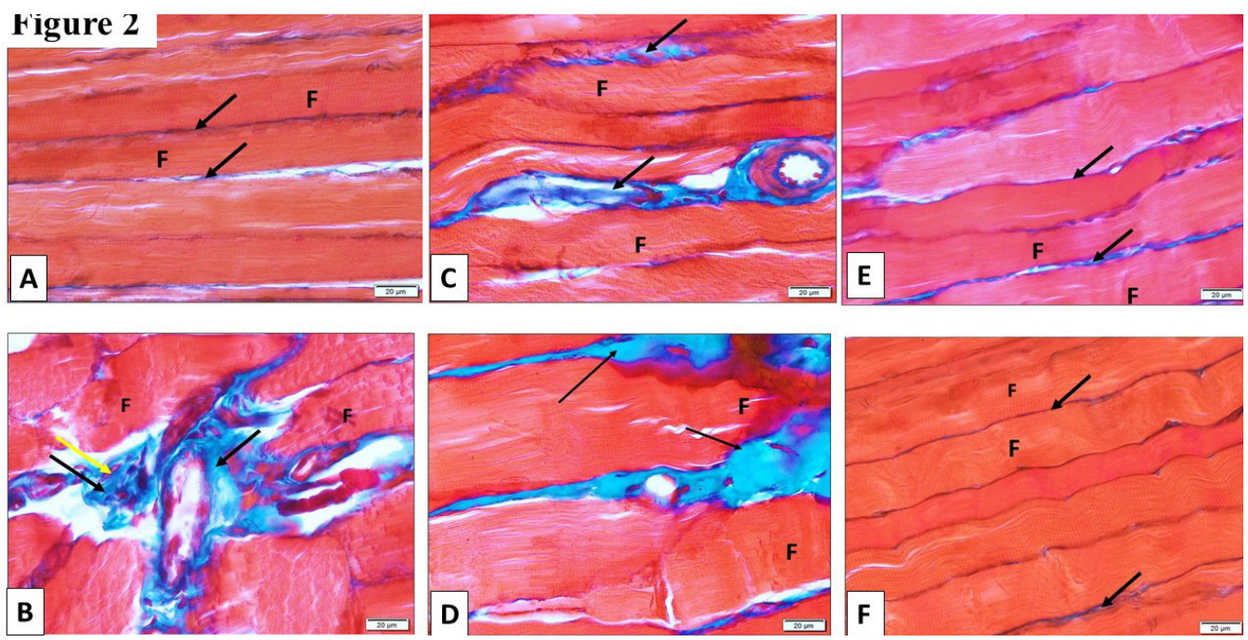

Fig. 2: Photomicrograph of a longitudinally cut section of gastrocnemius muscle stained with Masson Trichrome (x400). (2A): Group I showing cylindrical parallel muscle fibers (F) of uniform thickness separated by minimal amount of connective tissue endomysium (black arrow). (2B): Group II showing disorganized fragmented and discontinued muscle fibers (F). The connective tissue endomysium appears increased and contains extravasated red blood cells (yellow arrow) and collagen fibers (black arrows). (2C) Subgroup IIIA showing wide areas of fibrous tissue endomysium (black arrows) between muscle fibers (F). (2D): Subgroup IIIB (Spontaneous recovery group after 14 days) showing large amount of fibrous tissue between disorganized muscle fibers (black arrows). (2E): subgroup IVA showing minimal fibrous connective tissue between muscle fibers (black arrow). (2F): Subgroup IVB (Treated group after 14 days) showing minimal fibrous tissue (F) between well-organized muscle fibers (black arrow).

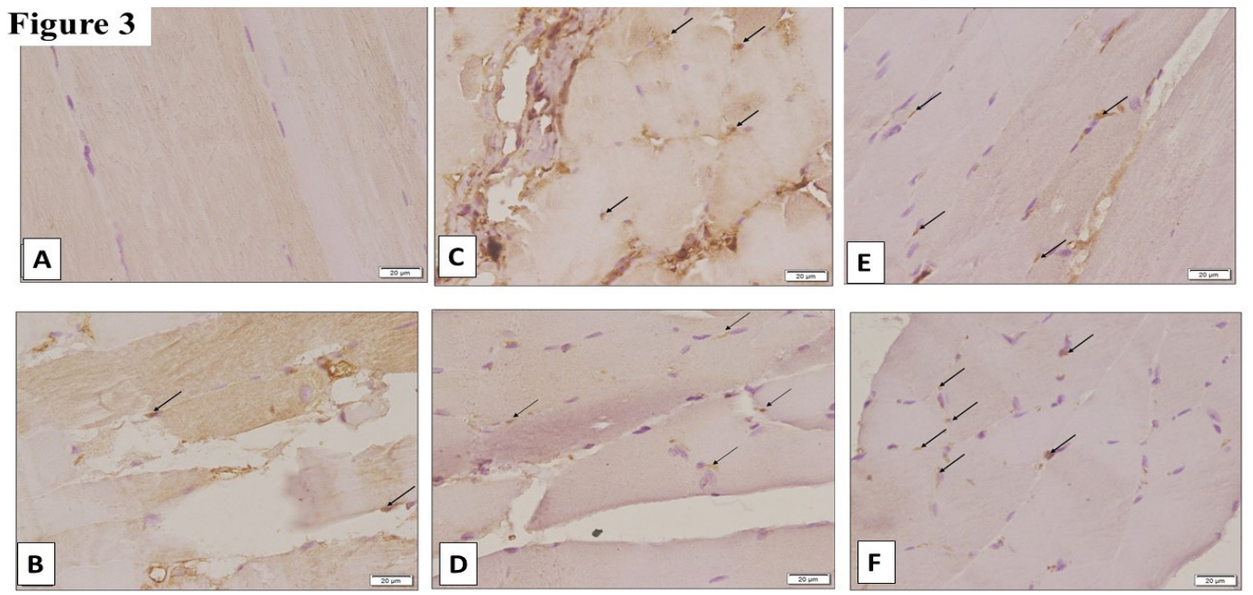

Fig. 3: Photomicrographs of a longitudinal section of gastrocnemius muscle stained with anti-myogenin antibody (x400). (3A): Group I showing negative nuclear immuno-staining in the vicinity of muscle fibers. (3B): Group II (Trauma group) showing occasional brown nuclei (black arrows) around the muscle fibers (3C): Subgroup IIIA (Spontaneous recovery group after 7 days) showing some immuno-stained nuclei (black arrows) around the muscle fibers. (3D): Subgroup IIIB showing many brown nuclei (black arrows) around the muscle fibers. (3E): Subgroup IVA showing many immuno-positive nuclei (black arrows) around the muscle fibers. (3F): Subgroup IVB showing large number of immuno-stained nuclei (black arrows) around the muscle fibers.

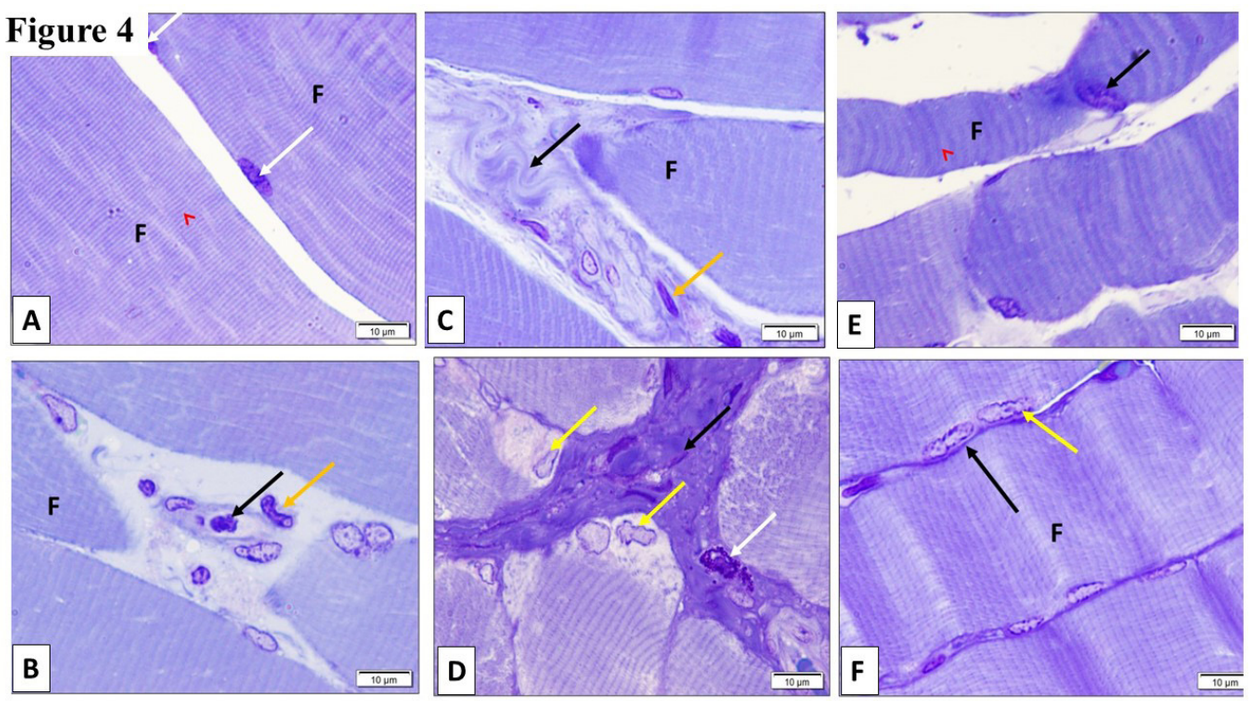

Fig. 4: Photomicrographs of a longitudinally cut semithin section of gastrocnemius muscle stained with toulidine blue (x1000). (4A): Group I showing parallel muscle fibers (F). Regular transverse striations (red arrowhead) across the whole thickness of the muscle fiber can be noted. Peripheral flat vesicular nuclei with prominent nucleoli (white arrows) are clearly observed. (4B): Group II showing tapering and discontinued muscle fiber (F). A blood capillary with a basophil (black arrow) in its lumen appears in increased CT as well as indented nuclei of macrophage (yellow arrow). (4C): Subgroup IIIA showing discontinued tapering muscle fiber with loss of transverse striations compared to control in some areas (F). The connective tissue endomysium shows excessive wavy collagen bundles (black arrow) and flattened oval nuclei of fibroblasts (yellow arrow). (4D): Subgroup IIIB showing muscle fibers with loss of striations in some areas, together with nuclei with irregular outline and paler compared to control in some areas (yellow arrows). Extensive fibrosis is seen in CT between muscle fibers (black arrow) with appearance of inflammatory cell as mast cell (white arrow). (4E): Subgroup IVA (showing some muscle fiber (F) with narrow diameter, central nucleus (black arrow) and coarse transverse striations (red arrowhead). (4F): subgroup IVB showing regularly arranged muscle fibers with transverse striations, festooned sarcolemma (black arrow) and peripheral flat vesicular nuclei with prominent nucleoli (yellow arrow).

Figure 5

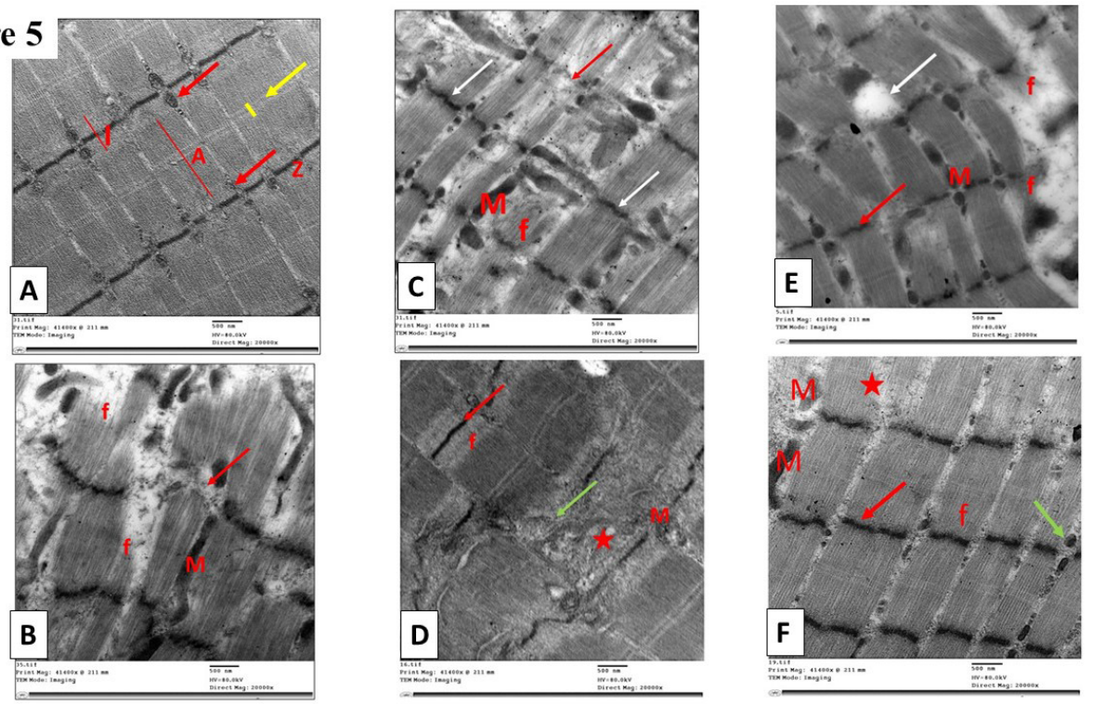

Fig. 5: Transmission Electron photomicrographs of longitudinally cut ultrathin section of an albino rat gastrocnemius muscle (x20000). (5A): Group I showing myofibrils with alternating dark (A) bands and light (I) bands. Each A band has a central H zone (yellow line) bisected by M line (yellow arrow). Each I band is bisected by a Z disc (Z). Sarcoplasm contains numerous intermyofibrillar mitochondria (red arrows). (5B): Group II showing discontinued muscle fibrils (f) with disorganized myofibrils completely lost Z discs (red arrow) appear at focal areas. Giant disfigured mitochondria (M) appear among the myofibrils. (5C): Subgroup IIIA showing occasional discontinued muscle fibrils (f), lost Z line (red arrow) and distorted mitochondria (M). Some other fibers appeared with intact Z line (white arrows). (5D): subgroup IIIB showing regular arrangement of muscle fibrils (f) with intact Z lines (red arrow) in some areas, while other areas show disorganized myofibril arrangement (red star) with disrupted Z line (green arrow). A mitochondrion (M) appears disfigured and giant among the myofibrils. (5E): Subgroup IVA showing intact Z lines in fibrils (red arrow). Discontinued muscle fibrils (f) are still recognized with many mitochondria between fibrils (M). Some areas still show complete dissolution (white arrow). (5F): Subgroup IVB showing regular arrangement of muscle fibrils (f) with intact Z line (red arrow) and regular mitochondria (green arrow) in some areas, while other areas still show disorganized myofibril arrangement (red star) with disrupted Z line. Mitochondria (M) appear disfigured and giant among the myofibrils.

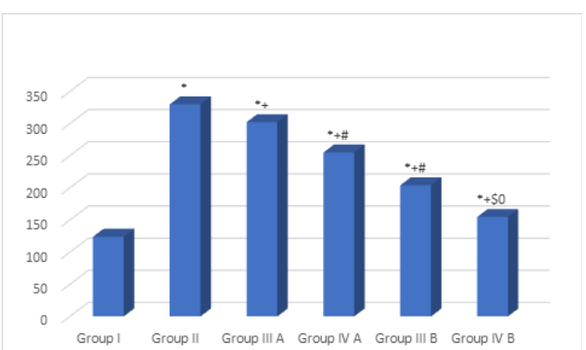

Histogram 1: Mean CPK level (± SD) among the studied Groups
*: Significant *P value* as compared to group I (*P*<0.05).
+: Significant *P value* as compared to group II (*P*<0.05).
#: Significant *P value* as compared to subgroup IIIA (*P*<0.05).
$: Significant *P value* as compared to subgroup IVA (*P*<0.05).
0: Significant *P value* as compared to subgroup IIIB (*P*<0.05).

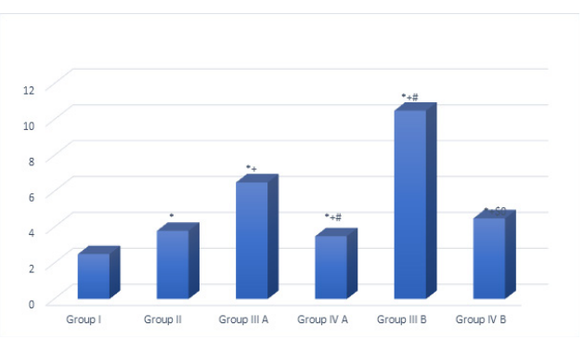

Histogram 2: Mean area percent of Masson trichrome (± SD)among the studied groups
*: significant *P* as compared to group I (*P*<0.05).
+: significant *P* as compared to group II (*P*<0.05).
#: significant *P* as compared to subgroup IIIA (*P*<0.05).
$: significant *P* as compared to subgroup IVA (*P*<0.05).
0: significant *P* as compared to subgroup IIIB (*P*<0.05)

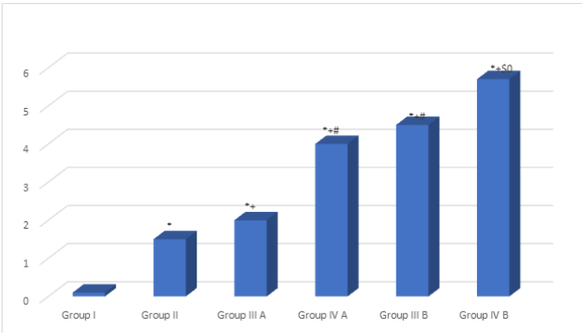

Histogram 3: Mean number ± SD of myogenin immunoreactive nuclei among the studied groups
*: Significant *P* as compared to group I (*P*<0.05).
+: Significant *P* as compared to group II (*P*<0.05).
#: Significant *P* as compared to subgroup IIIA (*P*<0.05).
$: Significant *P* as compared to subgroup IVA (*P*<0.05).
0: Significant *P* as compared to subgroup III B (*P*<0.05).

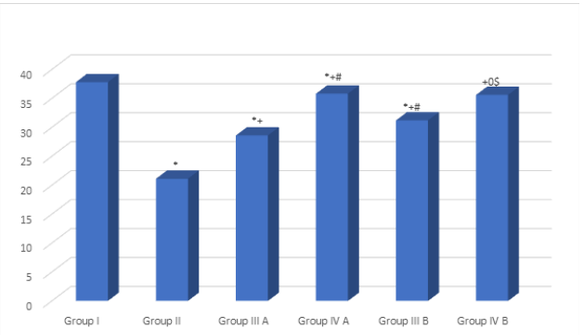

Histogram 4: Mean diameter (± SD) of muscle fibers among the studied groups
*: Significant *P* as compared to group I (*P*<0.05).
+: Significant *P* as compared to group II (*P*<0.05).
#: Significant *P* as compared to subgroup IIIA (*P*<0.05).
$: Significant *P* as compared to subgroup IVA (*P*<0.05).
0: Significant *P* as compared to subgroup IIIB (*P*<0.05).

DISCUSSION

Traumatic skeletal muscle injuries are widespread, that result in malfunction of the crushed muscle[19]. Usually, practicing pre-injury activities takes months, while preeminent fibrous scar replaces injured muscle tissue. The presence of the scar causes a decrease in muscle force, that can't contract, moreover scar location is susceptible to recurrent injury[20].

Regenerative medicine has used widely PRP especially in orthopedic sport- medicine. Several studies indicate profound impacts of PRP on the musculoskeletal system[21]. Consequently, the present study aims at studying the prospected function of PRP in repairing induced severe skeletomuscular crush injury in the test rats.

Often, the gastrocnemius muscle is subjected to severe injury during practicing many sports[22], therefore, the present study was mainly concerned in it. The experiment duration was classified into two phases; 7 days[11,23] and 14 days[14] to compare the results of muscle tissue damage and the possible function of PRP in muscle damage repair over short and long durations.

The present experimental results indicate that CPK mean-values in Group I were remarkably increased compared with the control. This could be explained by that muscle membrane-cells exhibited extensive damage when the muscle acutely injured, this membrane damage was severe enough to permit the uncontrolled efflux of cytosolic proteins from the muscle, including creatine kinase[24].

The CPK is an enzyme having important function in buffering ATP, that extends the duration of activity in skeletal muscles. Also, It plays a significant part in directing energy demand from ATP breakdown sites to the mitochondria. So, CPK is inspected in blood tests as a marker of tissue damage rich in creatine kinase such as in myositis and rhabdomyolysis[25].

Examination of sections from gastrocnemius muscle obtained from group II (Trauma group) revealed disorganized, discontinued, as well as tapering muscle fibers. Attenuation and tapering of muscle fibers was confirmed statistically, where the mean diameter was significantly reduced when compared to control. In addition, connective tissue endomysium appeared widened and contained apparently numerous CT fibers as well as cells. Capillaries with leucocytes inside their lumen, mainly basophils and macrophages, appeared in the widened CT while the mean area percent of sections stained with Masson trichrome was significantly increased compared to control.

These findings could be interpreted by immediate hematoma formation between the damaged myofibers with clear debris following muscle injury, then, inflammatory cells, in particular phagocytic macrophages rapidly infiltrate them. Simultaneously, activated fibroblasts synthesize numerous growth factors and extra-cellular matrix (ECM) components as fibronectin, collagen I and III and proteoglycans. The connective tissue continues to expand due to cell migration and proliferation[26]. The ECM deposition is regulated by transforming growth factor (TGF), connective tissue growth factor, and the renin-angiotensin system[27]. This ECM serves as a framework for the regenerated myofibers, it offers a sufficient environment for myoblast development[28]. Moreover, a key element of the ECM known as collagen VI controls the function of satellite cells (SCs) and preserves the SC pool throughout regeneration[29]. Moreover, when muscle regenerates following damage, SCs and fibroblasts interact favorably[30].

Ultrathin sections examined by TEM from Group II confirmed muscle degeneration in the form of discontinued muscle fibrils with disorganized myofibrils and occasional disrupted or completely lost Z discs appeared at focal areas. Z-disk deformations are probably due to forces transmitted through filaments, not only through passive elements as titin and desmin[24]. Also, the results illustrate giant disfigured

mitochondria in muscle cells whose production associated with a dysfunction of respiratory chain complexes has been involved in many diseases. Mitochondria have a major role in apoptosis, presumed to be implicated in the myocyte loss. The mitochondria - a special category known as megamitochondria- appears in different diseases or stress conditions. Cristae change their plane-parallel organization to tubular convoluted structures[31]. Regarding myogenin immunostained sections of group II (Trauma group) showed increase in mean number of myogenin immunopostive nuclei compared to control. It has been reported[32,33] that muscle injury activates SCs to divide and differentiate to specialized myogenic cells stained with myogenin.

After 7 days, mean values of serum CPK of subgroup IIIA were significantly increased compared with the control. The amount of uncontrolled influx of cytosolic calcium corresponds to value of following leakage of cytosolic proteins into the extracellular space, proposing that increase in membrane injury probably is controlled by calcium[34]. Also, next days of muscle injury, the amount of muscle cytosolic proteins in extracellular space increases progressively. That suggests that majority of the cell membrane damage resulted from muscle injury is caused by secondary factors to mechanical damage[24].

Subgroup IIIA (Spontaneous recovery group) showed irregularly arranged muscle fibers with frequent splitting which was associated with significant increase in mean diameter of skeletomuscular fibers in comparison to group II. Such splitting of muscle fibers is a response for adaptation, occurring when the fiber achieves a crucial size where oxygen and metabolites trade are inadequate[35]. Examination by TEM confirms these findings, it shows occasional discontinued muscle fibrils, lost Z-lines and distorted mitochondria, that denotes further muscle damage.

The connective tissue showed excessive fibrous tissue with mononuclear cellular infiltration and flattened oval nuclei of fibroblasts that was confirmed by mean area percent of Masson trichrome-stained sections where the mean area percent of fibrous tissue was significantly increased compared with control and group II. Muscle fibrosis ordinarily occurs after muscle injury and the function and structure properties of skeletal muscle becomes worse, that affects muscle fiber regeneration after injury[36]. Also, it promotes muscle reliability to re-injury[37].

Muscle fibrosis is closely related to inflammation. When muscle is injured, neutrophils are involved in the damage position to phagocytose injured cells and start regeneration[38]. These neutrophils release chemo-attractant cytokines, which stimulate more infiltration of monocytes and macrophages[39]. Macrophages have two heterogeneous phenotypes that take a vital part in fibrosis. The activated M1-phenotype produces proinflammatory cytokines, resulting in activating the fibroblast proliferation[40]. The activated M2-subtype produces transforming growth factor-β1 (TGF-β1) and fibronectin. Transforming growth factor-β1 activates inhabitant fibroblasts and resides fibroadipogenic progenitors (FAPs) apoptosis and induces their differentiation into fibrogenic lineage causing increased ECM deposition and fibrosis[41]. The extraction of TGF-1 is increased by an imbalance between M1 and M2 macrophage activity, which in turn enhances muscle fibrosis[42].

Mean number of myogenin immunoreactive nuclei in subgroup IIIA was significantly higher than in group II (trauma group), that may be attributed to muscle damage as satellite cells are normally quiescent but are activated immediately after injury. Damaged-myofiber derived factors directly trigger SCs, causing them to initiate cell cycle. Nevertheless, because these cells have been reversed to a quiescent-like condition, many of them do not advance to S-phase[43].

Mean value of CPK of subgroup IVA (Treated Group) significantly decreased compared with subgroup IIIA indicating a decrease in muscle fiber damage.

Moreover, H. and E.-stained sections from the same group showed regularly arranged muscle fibers. Connective Tissue showed inflammatory cellular infiltrate as well as dilated congested blood vessels, where a combination of resident and infiltrating inflammatory cells is needed for the efficient healing of injured skeletal muscle[44].

Semithin sections showed muscle fibers having narrow diameter, central nucleus and transverse striations. These findings were confirmed by TEM which demonstrated intact Z lines in fibrils with many mitochondria between them.

The existence of faint central nuclei may propose starting of regeneration process in the focal areas. Satellite cells were activated responding to a muscle injury, then start proliferation; in that case, satellite cells are described as myoblasts which may form myotubules with central vesicular nuclei[45,46]. These nuclei are vesicular with prominent nucleoli and the regenerating fibers are characterized by large, clear nuclei and prominent nucleoli indicating vigorous transcriptional activity[47]. This was confirmed by increase in mean number of myogenin immunoreactive nuclei among this group compared with subgroup IIIA due to an increase in SCs and a decrease in mean value of CPK in comparison to subgroup IIIA indicating a reduction in muscle fiber damage, also there was large increase in mean diameter of muscle fiber compared with group IIIA which did not receive PRP.

Karpati and Molnar (2008)[48] explained that during the regenerative process, myoblasts were found to be rich in mitochondria and glycogen reflecting vigorous energy metabolism.

Growth factors included in PRP take a vital part in healing of muscle fibers. Injecting PRP in muscle injury shows profound consequence on fibers healing[49].

Statistical analysis revealed that the mean number of myogenin immunoreactive nuclei in subgroup IVA was significantly higher than subgroup IIIA. The reported explanation[50] is that applying PRP, which comprises various growth factors, stimulates the resident SCs at wound location. With the release of several substances, macrophages and SCs promote one another to break down necrotic tissue and multiply as myofiber precursors. Vascular endothelial growth factor (VEGF), the main growth factor causing angiogenesis, is more concentrated after PRP injection. Increased vascularization of damaged tissue cause improving the repairing process.

Mean area percent of Masson trichrome-stained CT was significantly lower than in subgroup IIIA. This conclusion is consistent with reported researches[51,52] indicating that injecting PRP alone or combined with antifibrosis agents can remove fibrous scars in the damaged skeletal muscles. These findings have been indicated by other researchers[23,50], who reported that growth factors and active proteins have a significant role in recovery of damaged tissues and the reduction of pain. The great effect of PRP on muscle -regeneration enhancement after injury has been proved, that was verified by promoting proliferation, activation, differentiation of satellite cells and restoration of normal structure of muscle fibers. It has been justified that the injection of PRP in muscle injury site has helpful outcome on healing[49].

After 14 days, sections of subgroup IIIB showed incomplete regeneration in the form of muscle fibers with relatively apparent small diameter and loss of striations in some areas, together with nuclei of irregular shape. The TEM also showed disorganized myofibril arrangement with disrupted Z lines and mitochondria appeared giant and disfigured among the myofibrils. In addition, connective tissue between muscle fibers showed extensive regular fibrosis which was confirmed statistically by mean area percent of Masson trichrome-stained fibrous tissue that was significantly the highest among all the other groups. This extensive fibrosis may the disorder of the balance between M1 and M2 macrophage activation, increasing the expression of TGF-β1, which activates resident fibroblasts and induces their differentiation into fibrogenic lineage leading to excessive ECM deposition and fibrosis following muscle injury[53].

After 14 days, mean CPK level of subgroup IVB (Treated group) was the lowest among all the other groups. Histological examination of subgroup IVB showed regression of the muscle damage. Parallel regularly arranged muscle fibers and peripherally arranged flat nuclei. Semithin and TEM examination confirmed muscle regeneration in the form of regularly arranged muscle fibers exhibiting clear transverse striations, peripheral flat vesicular nuclei with prominent nucleoli and festooned sarcolemma. Festooning of the sarcolemma seen in semithin sections has been explained by Ervasti in 2013[54] who stated that dystrophin is a large protein present within the muscle in a lattice form called a costameres. It is present at the Z disc to anchor the myofibrils to external laminin making this area less extensible. On exposure to forced muscle contraction or oxidative stress, the sarcolemmal lipid bilayer is exposed to tension which is minimized by costameres resulting in folding or festooning of the sarcolemma to minimize this stress.

The mean diameter of muscle fibers was higher than both subgroup IIIB and IVA. Moreover, the mean number of myogenin immunoreactive nuclei was the highest among all the other groups. Hammond *et al*. (2009)[55] explained that hepatocyte growth factor found in PRP could activate quiescent satellite cells and PRP was found to accelerate their activation and increase the diameter of the regenerating fibers.

It was proven that intramuscular injections of PRP bring several autologous growth factors at supraphysiological concentrations to injured location, affecting on cell migration, proliferation, differentiation, or fusion and eventually enhancing muscle regeneration and decreases inflammation and apoptosis of injured muscles[56].

CONCLUSION

Present results indicate that PRP enhances and promotes repairing of severe crushed skeletal muscle and accelerates the healing process with minimal fibrosis in albino rats, however, further clinical trials are recommended to establish their effect on patients and the healing efficiency should be evaluated after longer durations to assess the chance of injury recurrence specially in athletes.

CONFLICT OF INTERESTS

There are no conflicts of interest.

REFERENCES

1. Mosca M. J. and Rodeo S. A. (2015): Platelet-rich plasma for muscle injuries: game over or time out?', Current Reviews in Musculoskeletal Medicine. 8: 145–153.
2. Borrione P., Fossati C., Pereira M.T., Giannini S., Davico M., Minganti C. and Pigozzi F. (2018): The use of platelet-rich plasma (PRP) in the treatment of gastrocnemius strains: a retrospective observational study. Platelets. Taylor & Francis. 29: 596–601.
3. Andia I. and Abate M. (2013): Platelet-rich plasma: underlying biology and clinical correlates. Regen. Med. 8: 645–658.
4. Kon E., Filardo G., Di Martino A. and Marcacci M. (2010): Platelet-rich plasma (PRP) to treat sports injuries: evidence to support its use. Knee Surgery, Sports Traumatology, Arthroscopy. 19: 516–527.
5. Elghblawi E. (2017): Platelet-rich plasma, the ultimate secret for youthful skin relixir and hair growth triggering. J Cosmet Dermatol. 17: 423–430.
6. Kennedy M.I., Whitney K., Evans T. and LaPrade R.F. (2018): Platelet-rich plasma and cartilage repair. Current Review in Musculoskeletal Medicine. 11: 573–582.

7. Hunter C.W., Davis T. and Fadadu P. (2018): Advanced procedures for pain management. Anesthesia & Analgesia. 127: 443-456

8. Garciaa T.A., Camargob R.C.T., Koikeb T.E.,Ozakia G.A.T., Castoldia R.C. and Filhob J.C.S.C.(2017): Histological analysis of the association of low level laser therapy and platelet-rich plasma in regeneration of muscle injury in rats. Brazilian Journal of Physical Therapy. Associação Brasileira de Pesquisa e Pós-Graduação em Fisioterapia. 21: 425–433.

9. Faralli H. and Dilworth F.J.: (2012): Turning on Myogenin in Muscle. A paradigm for understanding mechanisms of tissue-specific gene expression, in comparative and functional genomics. 2012: 836374.

10. Ganassi M., Badodi S., Wanders K., Zammit P.S. and Hughes S.M.(2020): Myogenin is an essential regulator of adult myofibre growth and muscle stem cell homeostasis. Elife. 1: e60445.

11. Quarteiro M.L., Tognini J.R.F., Flores de Oliveira E.L. and Silveira I. (2015): The effect of platelet-rich plasma on the repair of muscle injuries in rats. Revista Brasileira de Ortopedia (English Edition). Sociedade Brasileira de Ortopedia e Traumatologia. 50 : 586–595.

12. Sonnleitner D., Huemer P., Sullivan D.Y. (2000): A simplified technique for producing platelet-rich plasma and platelet concentrate for intraoral bone grafting techniques: a technical note. Int J Oral Maxillofacial Implants. 15:879-82.

13. Filippin L.I., Cuevas M.J., Lima E., Marroni N.P., Gonzalez-Gallego J., Xavier R.M. (2011): Nitric oxide regulates the repair of injured skeletal muscle. Nitric Oxide - Biology and Chemistry. Elsevier Inc. 24: 43–49.

14. Terada S., Ota S., Kobayashi M., Kobayashi T., Mifune Y., Takayama K, Witt M., Vadal`a G., MD, Oyster N., Otsuka T., Fu F.H. and Huard J. (2013): Use of an antifibrotic agent improves the effect of platelet-rich plasma on muscle healing after injury. The journal of bone and joint surgery. 95: 980-8.

15. Pourghasem M., Nasiri E. and Shafi H. (2014): Early renal histological changes in Alloxan-induced diabetic rats. Int J Mol Cell Med. 3: 11-15.

16. Kiernan J.A. (2015): Histological and histochemical methods: Theory and practice. 5th edition, Scion Publishing, Banbury. P: 111-162.

17. Suvarna K., Layton C. and Bancroft J. (2013): Immunohistochemical techniques and Transmission electron microscopy In: Bancroft's Theory and practice of Histological Techniques, 7thedition, Elsevier Health Sciences, China: P: 381-426 and P: 492-538.

18. Emsely R., Dunn G. and White I.R. (2010): Mediation and moderation of treatment effects in randomized controlled trials of complex interventions. Stat Methods Med Res. 19: 237-270.

19. Sicherer S.T., Venkatarama R.S. and Grasman J.M. (2020): Recent Trends in Injury Models to Study Skeletal Muscle Regeneration and Repair. Bioengineering (Basel). 7: 76.

20. Novak M.L., Weinheimer-Haus E.M. and Koh T.J. (2014): Macrophage activation and skeletal muscle healing following traumatic injury. The journal of pathology. 232: 344-55.

21. Tischer T., Bode G., Buhs M., Marquass B., Nehrer S., Vogt S., Zinser W., Angele P., Spahn G., Welsch G.H., Niemeyer P. and Madry H. (2020): Platelet-rich plasma (PRP) as therapy for cartilage, tendon and muscle damage - German working group position statement. J Exp Orthop. 7: 64.

22. Barroso G. C. and Thiele E. S. (2015): Muscle injuries in athletes. Revista brasileira de ortopedia, 46: 354–358.

23. Badr, S. M., Elbakary R., Laag E. M., Sarhan N. I. and Elbakary N. A. (2019): Histological study of the effect of platelet rich plasma on experimentally induced skeletal muscles injury in adult male albino rats. Egyptian Journal of Histology. 42: 369-380.

24. Tidball J.G. (2011): Mechanisms of muscle injury, repair, and regeneration. Compr Physiol. 1: 2029-62.

25. Barclay C. J. (2017): Energy demand and supply in human skeletal muscle. Journal of Muscle Research and Cell Motility. 2017: P 1-13.

26. Serrano A.L. and Muñoz-Cánoves P. (2010): Regulation and dysregulation of fibrosis in skeletal muscle. Exp Cell Res. 316: 3050–3058

27. Serrano A.L. and Muñoz-Cánoves P. (2016): Fibrosis development in early onset muscular dystrophies: mechanisms and translational implications. Sem Cell Dev Biol. 64: 181–190.

28. Delaney K., Kasprzycka P., Ciemerych M.A. and Zimowska M. (2017): The role of TGF-β1 during skeletal muscle regeneration. Cell Biol Int 41: 706–715.

29. Urciuolo A., Quarta M., Morbidoni V., Gattazzo F., Molon S., Grumati P., Montemurro F., Tedesco F.S., Blaauw B., Cossu G., Vozzi G., Rando T.A. and Bonaldo P. (2013): Collagen VI regulates satellite cell selfrenewal and muscle regeneration. Nat Commun. 4:1964.

30. Murphy M.M., Lawson J.A., Mathew S.J., Hutcheson D.A. and Kardon G. (2011): Satellite cells, connective tissue fibroblasts and their interactions are crucial for muscle regeneration. Development138: 3625-37.

31. Vays V. B., Eldarov C. M., Vangely I. M., Kolosova N. G., Bakeeva L. E., and Skulachev V. P. (2014): Antioxidant SkQ1 delays sarcopenia-associated damage of mitochondrial ultrastructure. Aging. 6:140–148.

32. Yamada M., Sankoda Y., Tatsumi R., Mizunoya W., Ikeuchi Y., Sunagawa K. and Allen R.E. (2008): Matrix metalloproteinase-2 mediates stretch-induced activation of skeletal muscle satellite cells in a nitric oxide-dependent manner in Int. J. Biochem. Cell Biol. 40: 2183–2191.

33. Wilschut K.J., Gong W., Oishi P.E. and Bernstein H.S. (2015): Derivation of engrafting skeletal muscle precursors from human embryonic stem cells using serum-free methods in J Stem Trans Bio.1: 106.

34. Fredsted A., Gissel H., Madsen K. and Clausen T.(2007): Causes of excitation induced muscle cell damage in isometric contractions: Mechanical stress or calcium overload? Am J Physiol. 292: 2249-2258.

35. Hassan N.F., El- Bakry N.A., Shalaby N.M., Ghobara M.M. and Bayomi N.A. (2009): Histological study of the effect of simvastatin on the skeletal muscle fibers in albino rat and the possible protective effect of Coenzyme Q10. Egypt. J. Histol. 31: 216 – 226.

36. Delaney K., Kasprzycka P., Ciemerych M.A. and Zimowska M. (2017): The role of TGF-β1 during skeletal muscle regeneration. Cell Biol Int 41: 706–715.

37. Prazeres P.H.D.M., Turquetti A.O.M., Azevedo P.O., Barreto R.S.N., Miglino M.A., Mintz A., Delbono O. and Birbrair A. (2018): Perivascular cell αv integrins as a target to treat skeletal muscle fibrosis. Int J Biochem Cell Biol. 5: 109–113.

38. Bersini S., Gilardi M., Mora M., Krol S., Arrigoni C., Candrian C., Zanotti S. and Moretti M. (2018): Tackling muscle fibrosis: from molecular mechanisms to next generation engineered models to predict drug delivery.Adv Drug Deliv Rev .129: 64–77.

39. Saclier M., Cuvellier S., Magnan M., Mounier R. and Chazaud B. (2013): Monocyte/macrophage interactions with myogenic precursor cells during skeletal muscle regeneration. FEBS J. 280: 4118–4130.

40. Ogle M.E., Segar C.E., Sridhar S. and Botchwey E.A. (2016): Monocytes and macrophages in tissue repair: implications for immunoregenerative biomaterial design. Exp Biol Med. 241: 1084–1097.

41. Lemos D.R., Babaeijandaghi F., Low M., Chang C.K., Lee S.T., Fiore D., Zhang R.H., Natarajan A., Nedospasov S.A. and Rossi F.M. (2015): Nilotinib reduces muscle fibrosis in chronic muscle injury by promoting TNF-mediated apoptosis of fibro/ adipogenic progenitors. Nat Med. 21: 786–794

42. Perandini L.A., Chimin P., Lutkemeyer D.D.S. and Camara N.O.S. (2018): Chronic inflammation in skeletal muscle impairs satellite cells function during regeneration: can physical exercise restore the satellite cell niche? FEBS J. 285: 1973–1984

43. Tsuchiya Y., Kitajima Y., Masumoto H. and Ono Y. (2020): Damaged myofiber-derived metabolic enzymes act as activators of muscle satellite cells. Stem Cell Reports. 15: 926-940.

44. Kharraz Y, Guerra J, Mann CJ, Serrano AL, Munoz-Canoves P (2013): Macrophage plasticity and the role of inflammation in skeletal muscle repair. Mediators Inflamm. 2013: 491-497.

45. Yoshida N., Endo J., Kinouchi K., Kitakata H., Moriyama H., Kataoka M. and Sano M. (2019): (Pro) renin receptor accelerates development of sarcopenia via activation of Wnt/YAP signaling axis. Aging cell. 18: e12991.

46. Tedesco F.S., Dellavalle A., Diaz-Manera J., Messina G. and Cossu G. (2010): Repairing skeletal muscle: regenerative potential of skeletal muscle stem cells. Journal of clinical investigation. 120: 11-19.

47. Greaves P., Chouinard L., Ernst H., Mecklenburg L., Pruimboom-Brees I.M., Rinke M., Rittinghausen S., Thibault S., Erichsen J.V. and Yoshida T. (2013): Proliferative and non-proliferative lesions of the rat and mouse soft tissue, skeletal muscle and mesothelium. J Toxicol Pathol. 26: 1S–26S.

48. Karpati G. and Molnar M.J. (2008): Muscle fibre regeneration. In human skeletal muscle diseases. 1st edition, Schiaffino S and Partridge T (eds.), Springer. P: 199-216.

49. Dzhyvak V., Klishch I., Datsko T. and Khlibovska O.(2020): Influence of PRP on morphological changes in muscle in the early period after traumatic muscle injury in the experiment. Journal of Education, Health and Sport. 10: 171-178.

50. Boivin J., Tolsma R., Awad P., Kenter K. and Li Y. (2021): The biological use of platelet-rich plasma in skeletal muscle injury and repair. Am J Sports Med. 14:1-9

51. Hamid M.S., Yusof A. and Mohamed Ali M.R. (2014): Platelet-rich plasma (PRP) for acute muscle injury: a systematic review. PLoS One.9:e90538.

52. Li H., Hicks J.J. and Wang L. (2016): Customized platelet-rich plasma with transforming growth factor b1 neutralization antibody to reduce fibrosis in skeletal muscle. Biomaterials.87: 147-156.

53. Perandini L.A., Chimin P., Lutkemeyer D.D.S. and Camara N.O.S. (2018): Chronic inflammation in skeletal muscle impairs satellite cells function during regeneration: can physical exercise restore the satellite cell niche? FEBS J. 285: 1973–1984

54. Ervasti J.M. (2013): Structure and function of the dystrophin-glycoprotein complex. In: Madame Curie bioscience database [internet]. Austin (TX): Landes bioscience. P 2000-2013.

55. Hammond J.W., Hinton R.Y., Curl L.A., Muriel J.M. and Lovering R.M. (2009): Use of autologous platelet-rich plasma to treat muscle strain injuries. Am J Sports Med. 37: 1135-1142.

56. Tsai W.C., Yu T.Y., Chang G.J., Chang H.N., Lin L.P., Lin M.S. and Pang J.S. (2021): Use of platelet-rich plasma plus suramin, an antifibrotic agent, to improve muscle healing after injuries. Am J Sports Med. 49: 3102-3112.

الملخص العربى

دراسة هستولوجية وهستوكيميائية مناعية للدور المحتمل للبلازما الغنية بالصفائح الدموية في إصلاح الإصابة الحادة المحدثة في العضلات الهيكلية لذكور الجرذان البيضاء البالغة

إيمي محمد أحمد[١]، سحر جمال أبو الفضل[١،٢]، داليا ابراهيم اسماعيل[١]، سهير أسعد فيلبس[١]

[١]قسم علم الأنسجة، كلية الطب، جامعة القاهرة

[٢]قسم الأنسجة الطبية ، كلية الطب ، جامعة مصر للعلوم والتكنولوجيا

خلفية: تعتبر إصابات الجهاز العضلي الهيكلي من أكثر الأسباب شيوعاً لمعظم إصابات الملاعب. العلاج الطبيعي التقليدي غير كافي أو مناسب للتعافي السريع. لذلك ، في هذه الدراسة ، تم فحص التأثيرات العلاجية للبلازما الغنية بالصفائح الدموية (PRP) على إصابة العضلات الهيكلية المستحثة في ذكور الجرذان البيضاء البالغة حيث أنها طريقة بسيطة وفعالة وتتطلب حداً أدني للتدخل الجراحي وتقلل وقت الشفاء.

مواد و طرق البحث: شملت الدراسة الحالية أربعة وخمسين من ذكور الجرذان البيضاء البالغة؛ قُسمت الي أربعة مجموعات: مجموعة (١) (المجموعة الحاكمة) , مجموعة (٢) (مجموعة الإصابة) تعرضت لإصابة سحق بعضلة الساق اليمني ثم ذُبحت بعد ساعتين, مجموعة (٣) (مجموعة التعافي التلقائي) لم تعالج وقُسمت لمجموعتين فرعية (٣ . ا) و (٣.ب) يشمل كل منها ٦ جرذان ذبحت بعد ٧ أيام و١٤ يوم على التوالي، مجموعة (٤) (المجموعة المعالجة) حُقنت ب ٠,١ مليلتر بالبلازما الدم الغنية بالصفائح الدموية في مكان الإصابة فور حدوثها. قسمت مجموعة المعالجة الي مجموعتين فرعيتين (٤.ا) و (٤.ب)، اشتملت كل منها ٦ جرذان، ذُبحت بعد ٧ أيام و١٤ يوم على التوالي. حُللت عينات الدم لتعين مستوي كرياتين فسفوكينيز. تم تشريح الجزء الأوسط من عضلة الساق واستؤصلت عينات منه للتقديرات للفحص الهستولوجي باستخدام هيموتوكسلين وإيوسين، وصبغة ماسون ثلاثية، والأجسام المضادة للميوجنين كدلالة للكشف عن الخلايا الرديفة في أنسجة العضلة المتجددة، ، وفحص الشرائح الدقيقة والمتناهة في الدقة باستخدام المجهر الضوئي والإلكتروني، وتبع ذلك الدراسات القياسية والإحصائية.

النتائج: أظهرت الدراسة وجود تشوه في الميتوكوندريا خلال الليفيات العضلية وصاحب ذلك ارتفاع عالي لكل من مستوي كرياتين فسفوكينيز والنسبة المئوية للمساحة المتوسطة للماسون ثلاثي الألوان والعدد المتوسط للأنوية الإيجابية للميوجينين، بينما قل كثيراً قطر ألياف العضلة بالمقارنة بالمجموعة الحاكمة. فحص شرائح الهيماتوكسيلين والأيوسيين و الشرائح الدقيقة للمجموعة (٢) أظهر ألياف عضلية غير منتظمة مجزأة وغير مستمرة. وأظهر اختبار الشرائح المتناهية السمك باستخدام المجهر الإلكتروني عضلة متليفة مقطعة مع ليفيات عضلية غير منتظمة كما ظهر تمزق عرضي أو فقد كامل لأقراص زد في المساحات المركزية. أظهرت المجموعة (٣) نقص في مستوي بلازما الدم الغنية بالصفائح الدموية وتحسن جزئي للضرر الحادث بألياف العضلة. أظهرت المجموعة (٤) تحسن ملحوظ للعضلة.

الاستنتاج: بلازما الدم الغنية بالصفائح الدموية تحسن وتعزز ترميم اصابات العضلات الهيكلية الحادة وتسّرع من عملية المعافاة من الإصابة بأقل تليف في أنسجة العضلة.